

NEUTRINOS FROM EARLY-PHASE, PULSAR-DRIVEN SUPERNOVAE

J.H. Beall ^{1,2,3} & W. Bednarek ⁴

ABSTRACT

Neutron stars, just after their formation, are surrounded by expanding, dense, and very hot envelopes which radiate thermal photons. Iron nuclei can be accelerated in the wind zones of such energetic pulsars to very high energies. These nuclei photo-disintegrate and their products lose energy efficiently in collisions with thermal photons and with the matter of the envelope, mainly via pion production. When the temperature of the radiation inside the envelope of the supernova drops below $\sim 3 \times 10^6$ K, these pions decay before losing energy and produce high energy neutrinos. We estimate the flux of muon neutrinos emitted during such an early phase of the pulsar - supernova envelope interaction. We find that a 1 km² neutrino detector should be able to detect neutrinos above 1 TeV within about one year after the explosion from a supernova in our Galaxy. This result holds if these pulsars are able to efficiently accelerate nuclei to energies $\sim 10^{20}$ eV, as postulated recently by some authors for models of Galactic acceleration of the extremely high energy cosmic rays (EHE CRs).

¹E.O. Hulburt Center for Space Research, Naval Research Laboratory, Washington, DC 20375

²Center for Earth Observing and Space Research, School for Computational Sciences, George Mason University, Fairfax, VA 22030

³St. John's College, Annapolis, MD 21404, USA

⁴Department of Experimental Physics, University of Łódź, ul. Pomorska 149/153, PL 90-236 Łódź, Poland

1. Introduction

The production of neutrinos with different energies during supernova explosions has been discussed extensively during the last several years, mainly in the context of gamma-ray bursts (GRBs). For example, neutrinos with energies > 100 TeV can be produced in the interactions of protons accelerated by a fireball shock with GRB photons (e.g. Waxman & Bahcall 1997, Vietri 1998). TeV neutrinos can arise in interactions of protons with radiation when the fireball jet breaks through the stellar envelope (Meszaros & Waxman 2001). GeV neutrinos can also be produced in the interactions of protons with neutrons which can be present in the fireball models discussed by Derishev et al. (1999) and Meszaros & Rees (2000).

Of course, the acceleration of particles to high energies is also expected in the case of classical supernovae. Recently, Waxman & Loeb (2001) estimated the neutrino flux from a Type II supernova when the shock breaks out of its progenitor star. Berezhinsky & Pritulsky (1978) and Protheroe, Bednarek & Luo (1998) have estimated the flux of neutrinos produced by particles accelerated by the young pulsar during the early phase of the supernova explosion (see also the calculations for the Crab Nebula case in Bednarek & Protheroe 1997).

In this paper we show that neutrinos can also be produced soon after the pulsar formation inside the supernova envelope and that these neutrinos are detectable by current neutrino detectors. As shown by Blasi, Epstein & Olinto (2000, BEO) or De Gouveia Dal Pino & Lazarian (2000), among others, particles can be accelerated to very high energies within the “plerion-like” region of a supernova shortly after the formation of the neutron star. We consider the scenario in which iron nuclei accelerated above the light cylinder of the pulsar interact: first, with the thermal radiation of the expanding supernova envelope, and later, with the matter of the envelope. Acceleration of hadrons in the pulsar wind zone has been discussed in the context of the production of high energy cosmic rays since shortly after the discovery of pulsars (e.g. Gunn & Ostriker 1969, Karakula, Osborne & Wdowczyk 1974). For likely parameters of pulsars at birth, we predict that the flux of muon neutrinos can be observable by large-sized neutrino detectors during about one year after supernova explosion.

2. The physical scenario

We consider type Ib/c supernovae, whose progenitors are Wolf-Rayet type stars. Such stars evolve from massive stars with $M \geq 35 M_{\odot}$, and create iron cores surrounded by relatively light envelopes of the order of a few solar masses. We use the models for the evolution of such stars and their explosions as published by Woosley et al. (1993). As an example, we concentrate on their model 60 WRA. The iron core collapses to a very hot proto-

neutron star which cools to the neutron star during about $t_{\text{NS}} \approx 5 - 10$ s from the collapse (Burrows & Lattimer 1986, Wheeler et al. 2000). The rest of the mass of the presupernova (the envelope) is expelled with the velocity at the inner radius of the order of $v_1 = 3 \times 10^8$ cm s^{-1} . However because of the density gradient, the outer parts of the envelope move faster. We approximate the velocities of matter in the envelope by the profile

$$v(R) = v_1(R/R_1)^b, \quad (1)$$

where the parameter $b = 0.5$ is obtained from an approximation of the velocity profile in the expanding envelope shown in Fig. 9 in Woosley et al. (1993), and we use $R_1 = 3 \times 10^8$ cm as the inner radius of the envelope at the moment of explosion. The density of matter in the envelope just before the collapse of the iron core can be approximated by the profile

$$n(R) = n_1(R/R_1)^{-a}, \quad (2)$$

where the density at R_1 is $n_1 = 1.2 \times 10^{31}$ cm^{-3} , and the parameter $a = 2.4$ is obtained from Fig. 1 in Khokhlov et al. (1999) by interpolation of the profiles for the radius and density versus the mass of the presupernova star (see also Fig. 3c in Woosley et al. 1993). The initial column density decreases with time, t , due to the expansion of the envelope according to

$$\rho(t) = \int_{R_1}^{R_2} n(R) \left(\frac{R}{R + v(R)t} \right)^2 dR, \quad (3)$$

where $R_2 = 3 \times 10^{10}$ cm is the outer radius of the envelope at the moment of explosion, and $v(R)$ and $n(R)$ are given by Eqns. 1 and 2, respectively. Just after the collapse of the iron core the temperature at the bottom of the envelope is $T_0 \approx 3 \times 10^9$ K at R_1 (see Fig. 8 in Woosley et al. 1993). Therefore the volume above the pulsar and below the expanding envelope is filled with thermal radiation which is not able to escape because of the high optical depth of the envelope. We apply that the temperature of this radiation drops with time during the expansion of the envelope according to

$$T(t) = T_0 \left(\frac{R_1}{R_1 + v_1(t_{\text{NS}} + t)} \right)^{3/4}. \quad (4)$$

At the moment of the neutron star's formation (after ~ 10 s), the temperature in the region below the envelope already drops to $\sim 5 \times 10^8$ K.

We assume that at this early age, the pulsar loses energy only via electromagnetic radiation. Therefore, its period changes according to the formula $P_{\text{ms}}^2(t) = 1.04 \times 10^{-9} t B_{12}^2 + P_{0,\text{ms}}^2$, where $P_{0,\text{ms}}$ P_{ms} are the initial and present periods of the pulsar (in milliseconds), and B_{12} is the pulsar surface magnetic field in units 10^{12} G. Note that after about 1 yr, the

pulsar may also lose efficiently energy on emission of gravitational radiation due to the r-mode instabilities which are excited in cooling neutron star (e.g. Andersson 1998, Lindblom, Owen & Morsink 1998). During this time, it is likely that the pulsar period changes suddenly reaching the value $\sim 10 - 15$ ms at about 1 yr after formation.

During the first year after explosion the rate of rotational energy loss by the pulsar is too low to influence the initial expansion velocity of the envelope (Ostriker & Gunn 1971), assuming that the pulsar has been born with parameters characteristic for the classical radio pulsars (e.g. the Crab pulsar). Only pulsars with periods of the order of a few milliseconds and super-strong magnetic fields (magnetars) can significantly accelerate the envelope at short time intervals after the explosion.

In the next section, we consider the acceleration of the iron nuclei in the pulsar magnetosphere above the light cylinder and below the expanding envelope, adopting the above model for the pulsar formation and expansion of the supernova envelope. Our aim is to find out if the acceleration and radiation processes inside the expanding envelope can produce an observable flux of neutrinos during the early phase of supernova explosion.

3. Acceleration of iron nuclei

Following the recent work by Blasi, Epstein & Olinto (BEO), we assume that the magnetic energy in the pulsar's wind zone accelerates iron nuclei close to the light cylinder radius in the mechanism called magnetic slingshot (Gunn & Ostriker 1969). Since this acceleration occurs very fast, the nuclei photo-disintegrate and lose energy during farther propagation in the radiation field below the supernova envelope (the cooling phase) but not during acceleration process. The energy that the iron nuclei can reach in the wind zone does depend on the pulsar parameters, so that

$$E_{Fe} = \frac{B^2(r_{LC})}{8\pi n_{GJ}(r_{LC})} \approx 1.8 \times 10^{11} B_{12} P_{ms}^{-2} \text{ GeV}, \quad (5)$$

where $r_{LC} = cP/2\pi$ is the light cylinder radius, and $n_{GJ} = B(r_{LC})/(2eZcP)$ is the Goldreich & Julian (1969) density at the light cylinder. As an example we show the temperature of the radiation field below the envelope of supernova and the energies of accelerated iron nuclei as a function of time in Fig. 1, in the case of two pulsars with parameters: $B_{12} = 4$, $P_{ms} = 3$, and $B_{12} = 100$, $P_{ms} = 10$. Note that in the case of the first pulsar, its period does not change, and consequently, the energies of the iron nuclei do not change significantly during the first year after the explosion. This is not the case for the second pulsar.

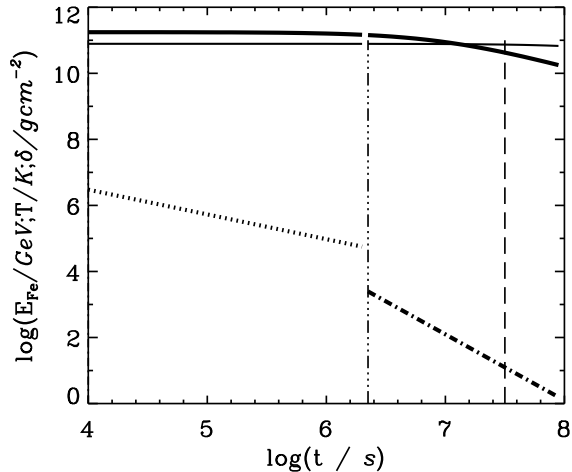


Fig. 1.— The dependences of the maximum energies of accelerated iron nuclei, the temperature of thermal radiation in the acceleration region (dotted curve), and the column density of matter in the envelope (thick dot-dashed curve) are shown as a function of time which is measured from the supernova explosion. Iron nuclei are accelerated by the pulsars with initial parameters: $B_{12} = 4$, $P_{\text{ms}} = 3$ (thin full curve) and $B_{12} = 100$, $P_{\text{ms}} = 10$ (thick full curve). The vertical lines mark the times: after which the envelope becomes transparent to thermal radiation (dot-dot-dot-dashed), and at which the envelope becomes transparent to hadronic collisions and the parameters of the neutron star may change drastically due to the gravitational energy losses (long dashed).

We obtain the spectrum of iron nuclei accelerated in the pulsar wind zone close to its light cylinder by following general prescription given by Blasi, Epstein & Olinto (BEO). In this simple model all nuclei are accelerated to the energy, E_{Fe} and their number is a part of the Goldreich & Julian density, $n = \xi n_{\text{GJ}}$. However, contrary to that work, we assume that the pulsar with specific parameters (B_{12} and P_{ms}) injects particles within some range of energies, due to the fact that the magnetic field at different parts of the light cylinder radius (and so the Poynting flux) is different. The magnetic field strength at the height h , measured from the plane containing the pulsar and perpendicular to the light cylinder radius, can be expressed by $B(r) \approx B(r_{\text{LC}}) \cos \alpha$, where $\cos \alpha = r_{\text{LC}} / (r_{\text{LC}}^2 + h^2)^{1/2}$. Therefore, the density of particles at the light cylinder $n(h) = n_{\text{GJ}} \cos^3 \alpha$, and their energies, $E = E_{\text{Fe}} \cos^3 \alpha$ depend on h . We calculate the number of particles injected at the height h per unit time from $dN/dt = 2\pi r_{\text{LC}} c n(h) dh$. Using the above formulae, we replace dh by dE and obtain the differential spectrum of iron nuclei injected by the pulsar at the fixed age of the pulsar, t ,

$$\frac{dN}{dE dt} = \frac{2\pi c \xi r_{\text{LC}}^2 n_{\text{GJ}}(r_{\text{LC}}) (E_{\text{Fe}} E^2)^{-1/3}}{3 [(E_{\text{Fe}}/E)^{2/3} - 1]^{1/2}} \cong \frac{3 \times 10^{30} \eta (B_{12} P_{\text{ms}}^{-2} E^{-1})^{2/3}}{[(E_{\text{Fe}}/E)^{2/3} - 1]^{1/2}} \frac{\text{Fe}}{\text{s GeV}}. \quad (6)$$

Note that our parameter ξ has similar meaning to the parameter ξ introduced by Blasi et al. (BEO). Due to the shape of the spectrum of iron nuclei $\propto E^{-1/3}$ (Eq. 6), also in our model most of the iron nuclei reaches the energies from the highest energy part of this spectrum at E_{Fe} , given by Eq. 5.

In this paper we discuss only the consequences of acceleration of iron nuclei at a relatively early phase after the supernova explosion, i.e up to about one year from pulsar formation. During this time, the radiation field inside the expanding supernova envelope, and thereafter, the column density of the envelope, are high enough to provide a target for relativistic nuclei. As we have already noted, the period of the neutron star can be significantly influenced by gravitational energy losses after about 1 year from the time of the explosion, when the neutron star cools enough.

4. Production of neutrinos

Accelerated nuclei move in the pulsar wind almost at rest in the wind reference frame (BEO). Therefore they do not lose significant energy by synchrotron emission. As we have noted, however, these nuclei will interact with the strong thermal radiation field in the supernova cavity, suffering multiple photo-disintegration of nucleons. Since the mean free paths for photo-disintegration of iron (and lighter) nuclei are significantly shorter than for their energy losses on e^\pm pair and pion production (see e.g. Karakula & Tkaczyk 1993),

the nuclei suffer complete disintegration onto nucleons before significant energy losses. For plausible parameters of the pulsar and the acceleration region, these secondary nucleons lose energy mainly via pion production. The pions then decay into high energy neutrinos if their decay distance scale $\lambda_\pi \approx 780\gamma_\pi$ cm, is shorter than their characteristic energy loss mean free path. The Lorentz factors of pions, γ_π , are comparable to the Lorentz factors of their parent protons, so they move similarly in the pulsar wind and their synchrotron losses should not dominate over their inverse Compton losses (ICS) in the thermal radiation. Pions lose energy on ICS process mainly in the Klein-Nishina (KN) regime, but not very far from the border with the Thomson regime. Therefore we can estimate the ICS losses of pions in the KN regime by

$$P_{\text{KN}}^{\text{ICS}} \approx 4/3\pi\sigma_T U_{\text{rad}}(m_e/m_\pi)^2\gamma_{\text{KN/T}}^2, \quad (7)$$

where σ_T is the Thomson cross section, U_{rad} is the energy density of radiation, m_e , m_π are the masses of electron and pion, and $\gamma_{\text{KN/T}} \approx 5 \times 10^{11}/T$ is the Lorentz factor at the transition between the KN and T regimes. We estimate the mean free path for pion energy losses via ICS

$$\lambda_{\text{ICS}} \approx m_\pi\gamma_\pi/P_{\text{KN}}^{\text{ICS}} \approx 10^{16}\gamma_\pi/T^2 \text{ cm}. \quad (8)$$

λ_{ICS} is comparable to the pion decay distance, λ_π , only for temperatures of radiation $T \leq 3 \times 10^6$ K. So then pions decay before significant energy losses only if this condition is fulfilled.

The temperature of the radiation inside the envelope drops to $T \leq 3 \times 10^6$ K at about $t_{\text{dec}} \sim 10^4$ s after the supernova explosion (see Eq. 4). At that moment nucleons from disintegration of nuclei cool in collisions with thermal radiation mainly by pion production. However, when the optical depth through the expanding envelope drops below $\sim 10^3$, the radiation is not further confined in the region below the envelope and its temperature drops rapidly. Based on Eqs. 1, 2, and 3, we have found that this happens at the time $t_{\text{conf}} \sim 2 \times 10^6$ s after the explosion (see the thin dot-dot-dot-dashed line in Fig. 1). Therefore, we conclude that nucleons are able to cool efficiently in the thermal radiation and produce pions, which then decay into muon neutrinos, but only from $t_{\text{dec}} \approx 10^4$ s up to $t_{\text{conf}} \approx 2 \times 10^6$ s after the explosion. At later times, the relativistic iron nuclei do not disintegrate in the radiation field but interact directly with the matter of the envelope whose density is already low enough so that pions produced by that interaction are able to decay into neutrinos and muons.

We now compute the differential spectra of muon neutrinos produced in the interaction of nuclei: (1) with the radiation field below the envelope during the period $1 \times 10^4 - 2 \times 10^6$ s after the supernova explosion; and (2) with the matter of the envelope during the period from $2 \times 10^6 - 3 \times 10^7$ s after the explosion, assuming that the nucleons cool to the lowest energies allowed by the column densities of photons and matter, respectively. In this calculation,

we assume that pions are produced in N- γ collisions with the Lorentz factors comparable to their parent nucleons. In the case of iron-matter (Fe-M) interactions, we apply the pion multiplicities given in Orth & Buffington (1976). As an example we show the results of these calculations (Fig. 2) for three pulsars with initial parameters: $P_{\text{ms}} = 3$ and $B_{12} = 4$ (model I, dashed histogram), $P_{\text{ms}} = 20$ and $B_{12} = 4$ (model II, dotted histogram), and $P_{\text{ms}} = 10$ and $B_{12} = 100$ (model III, full histogram). The iron nuclei accelerated by pulsars according to the models I and III fulfil the condition $P_{\text{ms}} \approx 4(B/10^{13}G)^{1/2}$ (given by BEO), which allow to reach energies 10^{20} eV. Note that even in the case of the model III, the energy losses of the pulsar during first year after its formation do not overcome the total kinetic energy of the envelope. Therefore the envelope is not accelerated. Model II describes the pulsar with the presumable parameters of the Crab pulsar at birth. The periods of pulsars in models I and II do not change drastically during the first year after the supernova explosion. However the period of the pulsar in model III changes by a factor of ~ 3 which causes the change in energy of the iron nuclei by about an order of magnitude during one year after explosion.

The numbers of neutrinos produced in these two processes do differ significantly, due to the fact that pion multiplicities in N- γ and Fe-M interactions are different. Therefore the neutrino fluxes from Fe-M interactions are up to an order of magnitude higher than the neutrino fluxes from N- γ interactions. Note also that the column density of the envelope after $\sim 2 \times 10^6$ s drops rapidly with time and only nuclei injected earlier than $\sim 10^7$ s can undergo multiple interactions with matter.

Since in model III the energies of accelerated iron nuclei significantly change during the first year it is interesting to investigate how the spectrum of neutrinos changes with time in this case. In Fig. 3 we show the spectra of neutrinos for the model III produced at different range of time after pulsar formation. The neutrino spectra have comparable intensities before $\sim 2 \times 10^6$ s after explosion (during N- γ production phase) with the cut-offs at this same energy (the pulsar period do not change significantly during this time see Fig. 1). However the location of the lower energy break in the neutrino spectra shifts with time to higher energies since it is determined by the temperature of radiation which drops with time. The highest fluxes of neutrinos are expected at $\sim 2 \times 10^6 - 10^7$ s after explosion during the interaction of iron nuclei with the matter of the supernova envelope. At later times ($10^7 - 3 \times 10^7$ s) the neutrino flux drops significantly, because particles, accelerated already to lower energies, are not completely cooled in collisions with the matter of the envelope (see Fig. 1).

Just after the collapse of the iron core, the column density of matter is high enough to absorb the neutrinos with energies above ~ 0.1 GeV. However, the column density drops quickly with time ($\propto t^{-2}$, see Eq. 4) and the cross-section for neutrino interaction with

matter increases with energy $\propto E_\nu$ and $\propto E_\nu^{0.4}$ below and above $E_\nu \sim 1$ TeV, respectively (e.g. Hill 1997). Therefore the optical depth becomes less than one at times $\sim 10^4$ s even for the highest energy neutrinos produced.

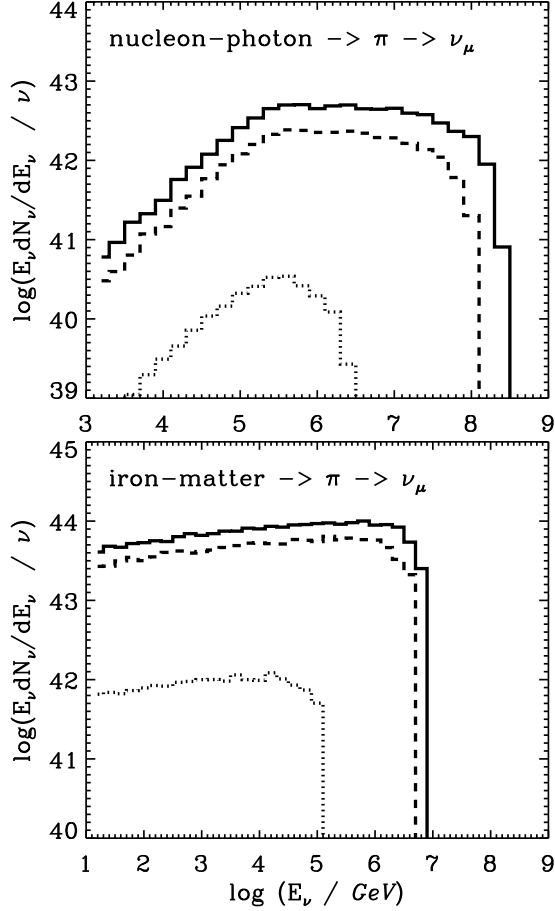


Fig. 2.— Spectra of muon neutrinos and antineutrinos produced in interactions of nucleons from photodesintegration of iron nuclei with the thermal radiation field inside the supernova envelope ($N - \gamma \rightarrow \pi \rightarrow \nu_\mu$) and from interactions of iron nuclei with the matter of the envelope ($Fe - M \rightarrow \pi \rightarrow \nu_\mu$). The density factor is $\xi = 1$, and the initial periods and the surface magnetic fields of the pulsars are: $P_{\text{ms}} = 10$ and $B_{12} = 100$ (full histograms), $P_{\text{ms}} = 3$ and $B_{12} = 4$ (dashed), and $P_{\text{ms}} = 20$ and $B_{12} = 4$ (dotted).

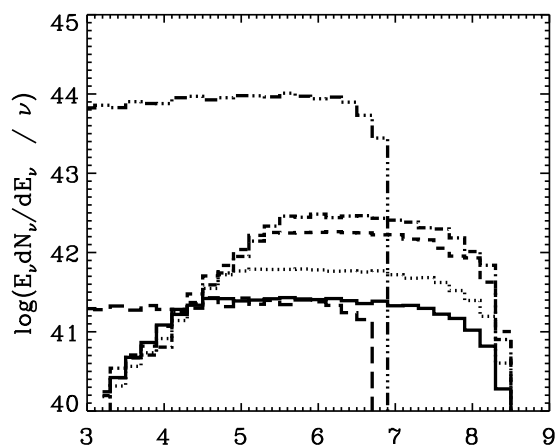


Fig. 3.— Spectra of muon neutrinos and antineutrinos produced by the pulsar with the parameters of the model III ($B_{12} = 100$, and $P_{\text{ms}} = 10$) at different range of time measured from the pulsar formation: $\Delta t = 10^4 - 10^5$ s (full histogram), $10^5 - 3 \times 10^5$ s (dotted), $3 \times 10^5 - 10^6$ s (dashed), $10^6 - 2 \times 10^6$ s (dot-dashed), $2 \times 10^6 - 10^7$ s (dot-dot-dashed), and $10^7 - 3 \times 10^7$ s (long dashed).

5. Discussion and conclusion

For a supernova inside our Galaxy at a distance, $D, = 10$ kpc, we estimate the expected flux of muon neutrinos produced (in nucleon-photon interactions during $1 \times 10^4 - 2 \times 10^6$ s after the explosion and produced in nuclei-matter collisions during $2 \times 10^6 - 3 \times 10^7$ s after the explosion) by integrating the neutrino spectra shown in Fig. 2. The likelihood of detecting these neutrinos by a detector with a surface area of 1 km^2 can be obtained using the probability of neutrino detection given by Gaisser & Grillo (1987). The results of our calculations, for the surface magnetic fields and initial periods of pulsars specified by the models I, II, III, and the density factor $\xi = 1$, are shown in Table 1 for the case of neutrinos arriving from directions close to the horizon, i.e. not absorbed by the Earth (H), and for neutrinos which arrive moving upward from the nadir direction and are partially absorbed (N) (for absorption coefficients see Gandhi 2000). We investigated in more detail the model III for which the time dependent neutrino spectra are calculated (see Figure 3). The expected, time dependent, number of neutrinos detected by 1 km^2 detector in this case for the horizontal and nadir directions are: 1.1×10^3 (H) and 250 (N) (at $\Delta t = 10^4 - 10^5$ s), 2.7×10^3 and 590 ($10^5 - 3 \times 10^5$ s), 7.9×10^3 and 1.7×10^3 ($3 \times 10^5 - 10^6$ s), 1.2×10^4 and 2.5×10^3 ($10^6 - 2 \times 10^6$ s), 1.8×10^5 and 6.4×10^4 ($2 \times 10^6 - 10^7$ s), 400 and 150 ($10^7 - 3 \times 10^7$ s). The highest detection rates of neutrinos are expected during about one-two months after supernova explosion from the phase of particle interaction with the matter of the envelope.

If EHE CRs are produced by pulsars within our Galaxy, than the observed flux of particles allows to constrain some free parameters of the considered model. By comparing the observed flux of cosmic rays at $\sim 10^{20}$ eV with model estimations of the flux of iron nuclei Blasi et al. (BEO) finds that following condition should be fulfilled $\xi \epsilon Q / \tau_2 R_1^2 B_{13} \approx 4 \times 10^{-6}$, where ξ is the efficiency for accelerating particles defined similarly as in our paper, ϵ is the fraction of pulsars which have the parameters required for particle acceleration to 10^{20} eV, Q is the trapping factor of particles within the Galactic Halo, $\tau = 100\tau_2$ yr is the rate of neutron star production, $R = 10R_1$ kpc is the radius of the Galactic Halo, and $B_{13} = 0.1B_{12}$ is the pulsar surface magnetic field. For plausible parameters: $\tau_2 = 1$, $R_1 = 3$ (required by the condition of isotropisation of EHE CRs), $Q \sim 1$ (see recent calculations of the propagation of hadrons within the Galaxy and Halo by Alvarez-Muniz, Engel & Stanev 2001, Bednarek, Giller & Zielińska 2001, and O’Neill, Olinto & Blasi 2001), and the rate of formation of neutron stars with required parameters equal to about 10% ($\epsilon = 0.1$), we obtain the limit on the particle acceleration efficiency $\xi \approx 10^{-4}$ for the model I, and $\xi \approx 4 \times 10^{-3}$ for the model III. These simple estimations combined with the results of our calculations of the numbers of expected neutrinos, presented in Table 1, show that some neutrinos might be observed in the 1 km^2 detector in the case of the pulsar described by the model I and a few hundred of neutrinos in the case of the model III. However, because of the steepness of the cosmic

ray spectrum such limits should be less restrictive for the pulsars accelerating particles to lower energies ($< 10^{20}$ eV). We conclude that the detection of neutrinos from early phase of supernovae (or lack, thereof) will put constraints on the recent models of extremely high energy cosmic ray production in supernova explosion with formation of very energetic pulsar (BEO; De Gouveia Dal Pino & Lazarian 2000).

It is clear from Table 1 that neutrinos from a Crab-type pulsar located at the distance of ~ 2 kpc (see our model II) might be observable by the 1 km^2 neutrino detector during the first year after pulsar formation if the particle acceleration efficiency is $\xi > 3 \times 10^{-3}$. Therefore it is likely that a recent explosion of a supernova at a distance similar to that of historical supernovae can also constrain the parameter ξ .

If the considered model works, then the whole population of pulsars created in the Universe should contribute to the extragalactic neutrino background. This could be detectable, because in such a case we do not need to be lucky to find the pulsar within the Galaxy during such an early phase. This interesting problem is considered in another paper (Bednarek 2001) in which we estimate the extragalactic neutrino background from the population of pulsars with parameters similar to those of classical radio pulsars formed in the Universe.

In fact, neutrinos can also be produced in later stages of supernova explosions, when the capturing of relativistic particles by the supernova envelope is efficient. Such scenarios have been considered in the case of proton acceleration in the pulsar’s wind zone (Berezinsky & Prilutsky 1978) and in the case of hadron acceleration in the pulsar inner magnetosphere (Bednarek & Protheroe 2001, Protheroe, Bednarek & Luo 1998). However, such a production of neutrinos is less certain, since it is expected that neutron stars can lose energy very efficiently via gravitational waves at about one year after explosion due to the r-mode instabilities. It has been argued that r-mode instabilities are not excited in the neutron stars with the surface magnetic fields typical for magnetars, i.e. $B \gg 10^{13}$ G (Rezzolla, Lamb & Shapiro 1999). Detection of neutrinos at these later times might militate against the r-mode instabilities as a means of the production of gravitational radiation. This in turn could have implications for the likelihood of detection of gravitational radiation associated with neutron star production. On the other hand, a sharp cutoff in the detected neutrino flux from a supernova could corroborate the existence r-mode instabilities and lend credence to the possibility of gravity wave generation and detection. Such a detection is of preeminent theoretical interest.

We are grateful to an anonymous referee for comments and suggestions which have improved the paper. WB thanks the the School for Computational Sciences (SCS) at George Mason University at Fairfax (Virginia) for hospitality during his visit. The research of WB was supported by the Polish KBN grant No. 5P03D 025 21.

Table 1: Expected number of detected ν_μ

	$P_{\text{ms}} = 3$ $B_{12} = 4$	$P_{\text{ms}} = 20$ $B_{12} = 4$	$P_{\text{ms}} = 10$ $B_{12} = 100$
N- $\gamma \rightarrow \nu_\mu$ (H)	8.4×10^3	2.6	2.4×10^4
Fe-M $\rightarrow \nu_\mu$ (H)	8.7×10^4	11.3	1.8×10^5
N- $\gamma \rightarrow \nu_\mu$ (N)	2×10^3	1.1	5.1×10^3
Fe-M $\rightarrow \nu_\mu$ (N)	3.4×10^4	8.6	6.4×10^4

REFERENCES

- Alvarez-Muniz, J., Engel, R., Stanev, T. 2001, Proc. 27th ICRC (Copernicus Gesellschaft 2001; Hamburg), p. 1972
- Andersson, N. 1998, ApJ, 502, 708
- Bednarek, W. 2001 A&A Lett., in press
- Bednarek, W., Giller, M., Zielińska, M. 2001, Proc. 27th ICRC (Copernicus Gesellschaft 2001; Hamburg), p. 1976
- Bednarek, W., Protheroe, R.J. 1997, PRL, 79, 2616
- Bednarek, W., Protheroe, R.J. 2001, Astropart.Phys., in press
- Berezinsky, V.S., Prilutsky, O.F. 1978, A&A, 66, 325
- Blasi, P., Epstein, R.I., Olinto, A.V. 2000, ApJ, 533, 123 (BEO)
- Burrows, A., Lattimer, J.M. 1986, ApJ, 307, 178
- De Gouveia Dal Pino, E.M., Lazarian, A. 2000, ApJ, 536, L31
- Derishev, E.V., Kocharovskiy, V.V., Kocharovskiy, Vl. V. 1999, ApJ, 521, 640
- Gaisser, T.K., Grillo, A.F. 1987, Phys.Rev. D, 39, 1481
- Gandhi, R. 2000, Nucl.Phys.Suppl., 91, 453
- Goldreich, P., Julian, W.H. 1969, ApJ, 157, 869
- Gunn, J., Ostriker, J. 1969, PRL, 22, 728
- Hill.G.C. 1997, Astropart.Phys., 6, 215
- Karakuła, S., Osborne, J.L., Wdowczyk, J. 1974, J.Phys. A, 7, 437
- Karakuła, S., Tkaczyk, W. 1993, Astropart.Phys., 1, 229
- Khokhlov, A.M. et al. 1999, ApJ, 524, L107
- Lindblom, L., Owen, B.J., Morsink, S.M. 1998, PRL, 80, 4843
- Meszáros, P., Rees, M.J. 2000, ApJ, 541, L5

- Meszaros, P., Waxman, E. 2001, PRL, submitted, astro-ph/0103275
- O’Neill, S., Olinto, A., Blasi, P. 2001 Proc. 27th ICRC (Copernicus Gesellschaft 2001; Hamburg), p. 1999
- Orth, C.D., Buffington, A. 1976, 206, 312
- Ostriker, J.P., Gunn, J.E., 1971, ApJ, 169, L95
- Protheroe, R.J., Bednarek, W., Luo, Q. 1998, Astropart. Phys., 9, 1
- Rezzolla, L., Lamb F.K., Shapiro, S.L. 2000, ApJ, 531, 139
- Vietri, M. 1998, PRL, 80, 3690
- Waxman, E., Bahcall, J. 1997, PRL, 78, 2292
- Waxman, E., Loeb, A. 2001, PRL, submitted (astro-ph/0102317)
- Wheeler, J.C., Yi, I., P. Höflich, L. Wang 2000, ApJ, 537, 810
- Woolsey, S.E., Langer, N., Weaver, T.A. 1993, ApJ, 411, 823